


Article

A Coordinated Mode Switch Control Strategy for a Two-Gear Power-Split Hybrid System

Qinpeng Sun ¹, Xueliang Li ², Xinlei Liu ² and Wei Wu ^{1,*} 

¹ School of Mechanical Engineering, Beijing Institute of Technology, Beijing 100081, China; sunqinpeng2024@163.com

² Hebei Key Laboratory of Special Equipment, Yanshan University, Qinhuangdao 066004, China

* Correspondence: wuweijing@bit.edu.cn; Tel.: +86-13810611647

Abstract: The hybrid system can extend the range of special vehicles and meet the electrical requirements of on-board equipment. In this paper, the driving force plummet problem of a new two-gear power-split hybrid system was studied during gear switches in a hybrid mode. The dynamic model of a hybrid electric system was established, and the effects of the engine angular acceleration and angular jerk on vehicle power and ride performance were obtained. The optimal ratio of the torque change rate of the motor and engine in the mode switch process was proposed. Considering the battery limitation and the external characteristics of the engine, the method of determining the target speed of the engine during shifting was proposed. Considering the response characteristics of each power source, the dynamic coordinated control strategy of multiple power sources in the mode switch process was proposed. The vehicle dynamics model was established based on the Matlab/Simulink 2020b and verified by simulation and a hardware-in-the-loop (HIL) test. The results show that the dynamic coordinated control strategy can reduce the peak impact by 80.33%, effectively improve the vehicle power and ride performance, and prevent the occurrence of high-current battery charging.

Keywords: power-split hybrid electric vehicles; mode switch; dynamic coordinated control strategy; impact control



Citation: Sun, Q.; Li, X.; Liu, X.; Wu, W. A Coordinated Mode Switch Control Strategy for a Two-Gear Power-Split Hybrid System. *Machines* **2024**, *12*, 427. <https://doi.org/10.3390/machines12070427>

Academic Editors: Ahmed Abu-Siada, Peter Gaspar and Junnian Wang

Received: 15 March 2024

Revised: 25 May 2024

Accepted: 6 June 2024

Published: 21 June 2024



Copyright: © 2024 by the authors. Licensee MDPI, Basel, Switzerland. This article is an open access article distributed under the terms and conditions of the Creative Commons Attribution (CC BY) license (<https://creativecommons.org/licenses/by/4.0/>).

1. Introduction

The generators and power battery in a hybrid system can ensure the vehicle's movement and meet the additional power demand of other on-board equipment at the same time. Compared with traditional fuel vehicles, hybrid vehicles have great advantages for fuel economy and emissions, which are valued by many countries and institutions [1]. With the advancement of electric motor technology in recent years, hybrid electric vehicles have achieved unprecedented development [2]. The hybrid system is mainly divided into series, parallel, and series-parallel systems in terms of configuration. Among them, the engine in a series-parallel system can be limited to work within an economic range, and the engine power can be directly used to drive the vehicle; therefore, it has a higher overall efficiency than the other two systems [3]. Compared with the series-parallel hybrid system using a single planetary gear, adding a two-gear automatic manual transmission (AMT) shift mechanism to the motor can significantly reduce the power demand of the hybrid system for the motor, and the vehicle power performance can be improved under high-speed conditions [4,5].

Due to the coupling of multiple power sources and the highly nonlinear and unpredictable characteristic of the engine in hybrid systems, significant changes in power distribution occur during a mode switch (which means the change in the hybrid vehicle's mode, such as changing from the electric vehicle mode to the hybrid electric vehicle mode or from a low gear to a high gear), resulting in a substantial impact on the vehicle dynamics [6–8]. Therefore, a dynamic coordinated control strategy (which means using the

dynamic control method to control the power source to coordinate the system to make a better comprehensive performance) is essential for effectively managing the system's dynamic response and ensuring optimal ride comfort [9,10].

For the demands of parallel hybrid systems, Qin Z et al. [11] developed a system to assist hybrid electric vehicles in maintaining a consistent speed while driving downhill, aiming to enhance safety. To address the limitations of previous studies, we propose an innovative dynamic coordinated control strategy for this downhill safety assistance system that considers its practical application. This strategy aims to ensure the overall system stability by focusing on both aforementioned aspects. Koprubasi K et al. [12] divided the mode switch process into multiple sub-states based on the state-space theory and designed a mode switch controller according to the different characteristics of each sub-state to reduce the power loss and impact of vehicles during a mode switch.

For the series-parallel hybrid system, due to the increase in the degrees of freedom in the system [13], impacts in the mode switch process are more common. So a dynamic coordination control strategy is widely used in the series-parallel hybrid system [14]. Due to the complex powertrain structure and various operation modes, torque fluctuations occur in the shifting process, which takes place during the synchronization of the gearshifts [15]. It is easy to cause torque fluctuations and vibration when driving, which greatly affect driving comfort. People have proposed many ways to overcome the disadvantages of the shifting process in a hybrid process [16,17]. Glielmo L et al. [18] proposed a hierarchical method based on cascaded and decoupled speed and torque control. Many scholars have introduced some advanced control methods into the coordinated control of the mode switch. For example, model predictive control (MPC) has attracted wide attention from engineers and has been applied in the control systems of plenty of powertrains in hybrid electric vehicles [19,20]. Beck R et al. [21] applied the MPC algorithm to the mode switch process of parallel hybrid vehicles to reduce the impact. The robustness of the proposed control strategy has been verified by the authors. Zeng X et al. [22] used a nonlinear observer to estimate the engine output torque, established an engine prediction model based on the MPC theory, and designed a feedback controller based on the expected value and actual value of the impact. As a result, the impact was reduced during the mode switch of the hybrid system. Tomura S et al. [23] designed an engine pulsation torque compensation controller and transmission output torque damping controller for the engine start-stop process of a Toyota THS hybrid system. The generator was used to actively compensate for the fluctuation of the engine output torque and the motor to compensate for the fluctuation of the transmission output torque. Wang Y et al. [24] proposed a heterogeneous network representation learning method, which improved the accuracy of the embedding results in the node classification task and had a great impact on identity recognition. Zhao J et al. [25] developed an innovative technique to design the output feedback optimal control (OFOC) of the continuous-time systems online, which could be adopted to performing online optimization of the input.

In this paper, the dynamic coordinated control problem among different power sources was studied for a new two-gear power-split hybrid system during the switch process from an HEV's low gear to an HEV's high gear. The dynamic performance and ride comfort of the vehicle and the charge and discharge limitation of the power battery were considered in the mode switch process. Based on the dynamic analysis and modeling of the hybrid system, the dynamic coordinated control strategy during the mode switch was proposed. The simulation results show that the proposed strategy can greatly improve the vehicle impact during the shifting process and the vehicle dynamic performance, and the adverse condition of a large current during power battery charging can be effectively avoided.

2. Overview of the Two-Gear Power-Split Hybrid System

2.1. The Two-Gear Power-Split Hybrid System Structure

The two-gear power-split hybrid system is composed of an engine, a generator, a motor, a coupling mechanism, a motor deceleration mechanism and a synchronizer. The

specific structure is shown in Figure 1. The engine and the generator are, respectively, connected with the carrier gear and the sun gear in the coupling mechanism (Planetary gear 1, PG1). The motor is connected with the sun gear in the motor deceleration mechanism (planetary gear 2, PG2). The ring gear in PG1 is fixed with the PG2 and the output shaft. The ring gear in PG2 is fixed with the coupling sleeve of the synchronizer 3, which could switch between housing and output shaft. Electric vehicle (EV) mode, hybrid electric vehicle (HEV) mode, parking charge mode and regenerative brake mode can be realized by controlling the start and stop of the engine and the states of the motor and the generator. Compared with the traditional single-gear power-split hybrid system, the PG2 can reduce the motor speed and increase the transmission output torque at low speed and large load. The maximum speed and maximum torque requirements for the motor is reduced and the vehicle dynamic performance is improved. In summary, the two-gear power-split hybrid system described in this paper can realize four driving modes: low-gear EV mode, low-gear HEV mode, high-gear HEV mode, and parking charge mode. The working status of each component in different modes are shown in Table 1.

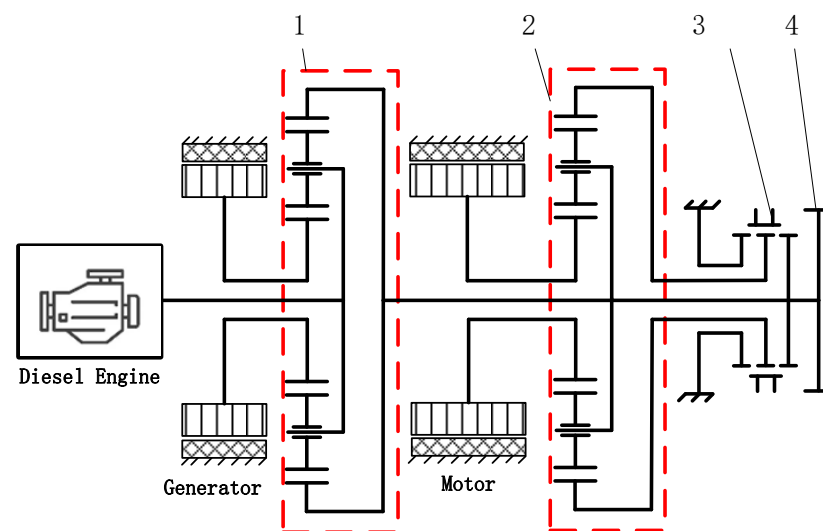


Figure 1. Two-gear power-split hybrid system. 1—Coupling mechanism. 2—Motor deceleration mechanism. 3—Two-gear AMT shift mechanism. 4—Main reducer input gear.

Table 1. Working statuses of all components in different modes.

Mode	Engine	Generator	Motor	Synchronizer
Low-gear electric vehicle (EV) pure electric mode	stop	idle	drive	← ¹
Low-gear HEV hybrid mode	start	power	drive	←
High-gear HEV hybrid mode	start	power/drive	drive	→
Parking charge mode	start	power	stop	←

¹ Note: “←” means the synchronizer coupling sleeve is in the left position (low-gear position), and “→” means the synchronizer coupling sleeve is in the right position (high-gear position).

2.2. The Control Strategy of the Two-Gear Power-Split Hybrid System

The transmission control unit (TCU) determines the states of all components during the vehicle is running by calculating factors such as demand power, state of battery (SOC), velocity, and the accelerator pedal position.

When the vehicle works in EV mode, the motor is powered by the power battery to provide all demand power. The motor target torque T_{Mreq} is calculated by TCU through drive demand for power and current motor speed, and it is sent to the motor control unit (MCU) to control its output torque. At the same time, the engine is off, and the generator is idle without torque outputting.

When the vehicle works in HEV mode, the engine and the power battery will provide power to drive the vehicle. At the same time, the TCU will allocate the power required by the engine and the power battery according to the SOC and the demand power by the drive, and calculate the target power of the engine P_{Ereq} and the target power of the power battery P_{Breq} . The engine target operating point is determined according to the calculated engine target power. The actual engine output speed is controlled by the engine control unit (ECU). The engine output torque is controlled indirectly by the generator control unit (GCU).

In addition, because of the maximum charge and discharge current limit of the power battery, the sum of the power of the generator P_G and the power of the motor P_M must be greater than the current maximum charging power P_{bcm} of the battery but less than the current maximum discharging power P_{bdcm} when ignoring the losses of the circuit and the two motors.

3. Shifting Process and Dynamic Analysis

3.1. Shifting Process Analysis

The two-gear power-split hybrid system described in this paper contains the following two different shifting processes: the up-shifting process in HEV mode and the down-shifting process in HEV mode.

In the shifting process, the motor needs to perform active speed regulation, so the synchronizer coupling sleeve needs to return to the middle position to release the motor from the transmission output shaft. In order to reduce synchronous ring wear and shifting impact, the output torque of the motor must be reduced to 0 when the synchronizer is released or combined. According to the working principle of HEV mode, the output torque of the transmission is provided by both the motor and the engine. When the output torque of the motor is rapidly reduced, the output torque of the transmission will also decrease rapidly. So it is necessary to increase the engine output torque to compensate the decrease torque of the output shaft of the transmission. In this process, if the output torque of the motor drops too fast or the engine does not rapidly increase the torque output in time, the output torque of the transmission will fluctuate violently. After the motor completes the active speed regulation, the synchronizer is engaged with left or right sides again. The transmission output torque will also fluctuate, if the motor regulated speed does not match the output speed or the engine does not reduce the torque output in a timely manner.

The above two situations will increase the shifting impact, and have a serious influence on the driving comfort and vehicle dynamic performance. Therefore, it is necessary to coordinate the output torque of the engine and the motor in order to eliminate power interruption and shifting impact during shifting in HEV mode. In addition, when the motor stops, the generator is still working. So the power battery charging power will increase rapidly with the torque of the engine ramping up. It is also necessary to control the power battery charging power during the shifting process to prevent the charging current from exceeding the limit of the battery.

3.2. System Dynamics Analysis of Shifting Process

The dynamics analysis is conducted on the vehicle, it can be known as:

$$\begin{cases} \dot{v}_{veh} = \frac{F_t - F_{res}}{m} \\ F_{res} = F_f + F_w + F_i \\ F_t = \frac{T_{wheel}}{r} = \frac{T_O i_0 \eta_0}{r} \end{cases} \quad (1)$$

where \dot{v}_{veh} is longitudinal acceleration of vehicle; F_t is vehicle driving force; m is vehicle mass; F_{res} is external resistance to the vehicle; F_f is ground rolling resistance; F_w is air resistance; F_i is slope resistance; T_{wheel} is total torque of the driving wheel; T_O is transmission output torque; i_0 is main reducer transmission ratio; η_0 is transmission efficiency of the main reducer; r is radius of the wheel.

The lever model of the coupling mechanism and decelerating mechanism of the motor in the two-speed power-split hybrid system is established to facilitate analysis of their internal dynamic relationship, as shown in Figure 2.

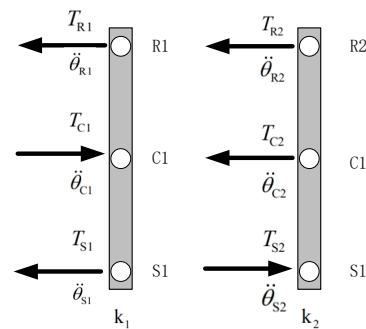


Figure 2. Lever model of coupling mechanism and reduction mechanism of motor.

In the figure, T_{S1} , T_{C1} and T_{R1} are, respectively, the torques of the sun gear, carrier gear and ring gear in the coupling mechanism. T_{S2} , T_{C2} and T_{R2} are, respectively, the output torque of the sun gear, carrier gear and ring gear in the motor deceleration mechanism; $\ddot{\theta}_{S1}$, $\ddot{\theta}_{C1}$ and $\ddot{\theta}_{R1}$ are the angular acceleration of the sun gear, carrier gear and ring gear of the coupling mechanism, respectively. $\ddot{\theta}_{S2}$, $\ddot{\theta}_{C2}$ and $\ddot{\theta}_{R2}$ are, respectively, the angular acceleration of the solar gear, carrier gear and ring gear in the motor deceleration mechanism; k_1 , k_2 are the characteristic parameters of the planetary gears of the coupling mechanism and the planetary gears of the decelerating mechanism of the motor, respectively.

The relationship between the speed of the transmission output shaft and the speed is as follows:

$$v_{\text{veh}} = \dot{\theta}_O i_0 r \quad (2)$$

where $\dot{\theta}_O$ is the transmission output shaft speed.

Since the transmission output shaft is fixed with the ring gear of the coupling mechanism and the carrier gear of the motor deceleration mechanism, there are:

$$\dot{\theta}_O = \dot{\theta}_{R1} = \dot{\theta}_{C2} \quad (3)$$

where $\dot{\theta}_{R1}$ and $\dot{\theta}_{C2}$ are, respectively, the speeds of the coupling planetary ring gear mechanism and the motor's decelerating mechanism's carrier gear.

Under different gears, due to the different combination state of the synchronizer, the output torque of the transmission is different, and the torque relationship for the output shaft of the transmission output shaft is as follows:

$$\begin{cases} T_{OL} = T_{R1} + T_{C2} \\ T_{ON} = T_{R1} \\ T_{OH} = T_{R1} + T_{S2} \end{cases} \quad (4)$$

where T_{OL} , T_{ON} and T_{OH} are the output torque of the transmission in low gear, neutral gear and high gear, respectively.

The inertia of each component in the planetary gear of the coupling mechanism is equivalent to that of the generator, engine and vehicle. And the inertia of each component in the planetary gear of the motor deceleration mechanism is equivalent to that of the motor and vehicle. For the planetary gear of the coupling mechanism and the deceleration mechanism of the motor, the output torque of each component and the torque relationship between each component are as follows:

$$\begin{cases} T_{S1} = T_G + J_G \ddot{\theta}_G \\ T_{C1} = T_E + J_E \ddot{\theta}_E \\ T_{S1} : T_{C1} : T_{R1} = 1 : -(1 + k_1) : k_1 \\ T_{S1} - T_{C1} + T_{R1} = 0 \end{cases} \quad (5)$$

$$\begin{cases} T_{S2} = T_M + J_M \ddot{\theta}_M \\ T_{S2} : T_{C2} : T_{R2} = 1 : -(1 + k_2) : k_2 \end{cases} \quad (6)$$

where T_E , T_G and T_M are, respectively, the output torque of the engine, generator and motor; $\ddot{\theta}_E$, $\ddot{\theta}_G$ and $\ddot{\theta}_M$ are the angular acceleration of engine, generator and motor, respectively. J_E , J_G and J_M are the moment of inertia of the engine, generator and motor, respectively.

The speed relationship of the components in the planetary gear of the coupling mechanism and the motor deceleration mechanism is as following:

$$\begin{cases} \dot{\theta}_{S1} + k_1 \dot{\theta}_{R1} - (1 + k_1) \dot{\theta}_{C1} = 0 \\ \dot{\theta}_{S2} + k_2 \dot{\theta}_{R2} - (1 + k_2) \dot{\theta}_{C2} = 0 \end{cases} \quad (7)$$

where $\dot{\theta}_{S1}$, $\dot{\theta}_{C1}$ are the speeds of the solar gear and the carrier gear in the planetary gear of the coupling mechanism, respectively. $\dot{\theta}_{S2}$, $\dot{\theta}_{R2}$ are, respectively, the rotation speed of the solar gear and the ring gear in the motor deceleration mechanism.

The time differential equations of the Equation (7) is as follows:

$$\begin{cases} \ddot{\theta}_G + k_1 \ddot{\theta}_O - (1 + k_1) \ddot{\theta}_E = 0 \\ \ddot{\theta}_M + k_2 \ddot{\theta}_{R2} - (1 + k_2) \ddot{\theta}_O = 0 \end{cases} \quad (8)$$

When the transmission is in low gear or high gear, the middle ring gear of the planetary gear of the motor reducer is, respectively, connected with the transmission housing or the output shaft, respectively, through the synchronizer. That is, $\ddot{\theta}_{R2} = 0$ at low gear or $\ddot{\theta}_{R2} = \ddot{\theta}_O = \ddot{\theta}_M$ at high gear. By combining Equations (1)–(8), the relationship among the vehicle acceleration, the output torque, and the angular acceleration of each power source can be solved under two different gear.

In low gear:

$$\dot{v}_{\text{veh}} - \frac{B_1}{A_1} \ddot{\theta}_E = \frac{1}{A_1} [T_E + T_G + (1 + k_2) T_M - \frac{r}{i_0} F_{\text{res}}] \quad (9)$$

In high gear:

$$\dot{v}_{\text{veh}} - \frac{B_1}{A_2} \ddot{\theta}_E = \frac{1}{A_2} [T_E + T_G + T_M - \frac{r}{i_0} F_{\text{res}}] \quad (10)$$

where $A_1 = [\frac{r}{i_0} m - J_M(1 + k_2)^2 + J_E k_1 \frac{i_0}{r}]$, $A_2 = [\frac{r}{i_0} m - J_M + J_E k_1 \frac{i_0}{r}]$, $B_1 = [J_G(1 + k_1) + J_E]$. Considering that the shifting process time is short, the speed will not change greatly, so the total driving resistance F_{res} can be considered as a constant. By differential Equations (9) and (10), the relationship between vehicle impact and the output torque change rate of the three power sources can be obtained.

In low gear:

$$\ddot{v}_{\text{veh}} - \frac{B_1}{A_1} \ddot{\theta}_E = \frac{1}{A_1} [\dot{T}_E + \dot{T}_G + (1 + k_2) \dot{T}_M] \quad (11)$$

In high gear:

$$\ddot{v}_{\text{veh}} - \frac{B_1}{A_2} \ddot{\theta}_E = \frac{1}{A_2} [\dot{T}_E + \dot{T}_G + \dot{T}_M] \quad (12)$$

According to Equations (9)–(12), the angular acceleration $\ddot{\theta}_E$ and angular jerk of the engine $\ddot{\theta}_E$ have great influence on the acceleration and impact control (which means to

use the dynamic coordinated control strategy to decrease the impact of the system) of the vehicle, respectively. If the speed of the engine changes rapidly in the shifting process, the angular acceleration of the engine may change rapidly. And the angular jerk of the engine may reach unreasonable values, affecting the effective control of the vehicle's acceleration and impact. Therefore, changes in engine speed during the shifting process should be minimized. Effective control of engine speed can be achieved by managing the generator output torque in order to maintain constant engine speed and zero angular acceleration and eliminate engine angular jerk. According to Equations (5) and (8), the relationship between engine angular acceleration, engine output torque, generator output torque and vehicle acceleration can be obtained as follows:

$$J_E \ddot{\theta}_E - J_G(1 + k_1)[k_1 \frac{\ddot{v}_{veh}}{r i_0} - (1 + k_1) \ddot{\theta}_E] = (1 + k_1) T_G - T_E \quad (13)$$

If the angular acceleration of the engine is constant, Equation (13) could be changed as follows:

$$T_E - (1 + k_1) T_G = J_G(1 + k_1) k_1 \frac{\ddot{v}_{veh}}{r i_0} \quad (14)$$

Considering that the inertia of the generator J_G and the longitudinal acceleration of the truck \ddot{v}_{veh} are small when the truck is fully loaded, the influence on the angular acceleration control of the engine can be ignored. In order to eliminate the influence of engine angular acceleration on vehicle acceleration control, it is necessary to adjust the output torque of the generator during shifting as follows:

$$T_G = \frac{1}{1 + k_1} T_E \quad (15)$$

Under the condition that the engine speed is controlled to a constant value, the angular jerk of the engine in Equations (11) and (12) can be ignored, so the two equations can be written as:

In low gear:

$$\ddot{v}_{veh} = \frac{1}{A_1} [\frac{k_1}{1 + k_1} \dot{T}_E + (1 + k_2) \dot{T}_M] \quad (16)$$

In high gear:

$$\ddot{v}_{veh} = \frac{1}{A_2} [\frac{k_1}{1 + k_1} \dot{T}_E + \dot{T}_M] \quad (17)$$

In order to achieve complete elimination of the shift impact during the shifting process, the relationship between the engine and the motor torque change rate should be as following two equations.

In low gear:

$$\frac{\dot{T}_E}{\dot{T}_M} = - \frac{(1 + k_1)(1 + k_2)}{k_1} \quad (18)$$

In high gear:

$$\frac{\dot{T}_E}{\dot{T}_M} = - \frac{(1 + k_1)}{k_1} \quad (19)$$

According to the above analysis, in order to completely eliminate the longitudinal impact of the vehicle during gear shifting, it is necessary to control the engine speed at a certain value and eliminate the influence of the engine angular acceleration, angular jerk and longitudinal impact on the longitudinal acceleration. In addition, in the process of reducing and ramping up the torque of the motor before and after shifting, the torque change rate of the engine and the motor should match the relationship of Equations (18) and (19).

3.3. Confirmation of the Shifting Process

In order to maintain the transmission's output torque and effectively control the vehicle impact during the shifting process from HEV low-gear mode to HEV high-gear mode, the control scheme of the upshift process is proposed as shown in Figure 3, which includes seven steps in the following three stages:

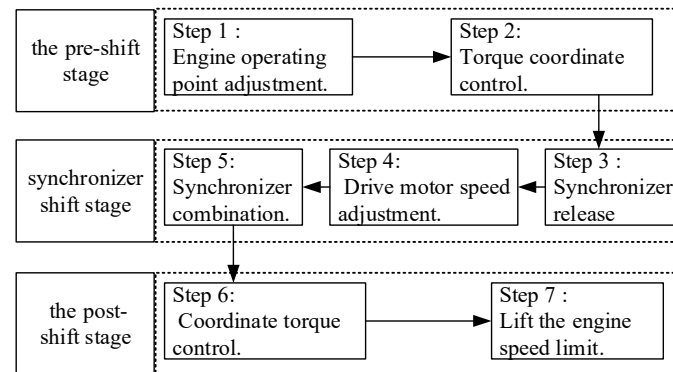


Figure 3. Up shift flow chart.

The first stage is the pre-shift stage, which is before the release of synchronizer. This stage is divided into two steps: engine target speed adjustment and dynamic coordinated control before the release of synchronizer.

Step 1 (Engine operating point adjustment): In order to keep enough adjustment time to make the engine speed change gently and prevent the engine output torque fluctuation caused by the rapid target speed change, the operating point of the engine should be adjusted in advance when the motor speed is close to the upshift speed threshold. In step one, the engine speed is adjusted to a set value and remains at that value during the shifting process.

Step 2 (Torque coordinate control. Before synchronizer release): In this step, the torque of the motor should be gradually reduced to 0. At the same time, it is necessary to increase the output torque of the engine to make up for the decrease in the output torque of the motor. The output torque of the both power sources is controlled to meet or approach the requirements of Equations (18) or (19). When the output torque of the motor is reduced to nearly 0, it is considered that the motor has completed unloading.

The second stage is synchronizer shift stage, which is divided into three steps: synchronizer release, motor active speed regulation and synchronizer combination.

Step 3 (Synchronizer release): The motor is released from the output shaft by controlling the shift motor drive coupling sleeve from the current position to the middle position.

Step 4 (Motor speed adjustment): The motor is controlled by active speed regulation. The goal is that the speed difference between the output shaft and the ring gear of the motor deceleration mechanism is eliminated, and the motor is unloaded after completion of synchronization.

Step 5 (Synchronizer combination): Similar to the third stage, the control shift motor drives the synchronizer combined with the sleeve to move from the middle position to the corresponding position of the next gear to complete the upshift.

The third stage is the post-shift stage, which is divided into two steps: dynamic coordinated control before synchronizer release and engine torque limit elimination.

Step 6 (Dynamic coordinated control after synchronizer combination): Similar to step 2, the purpose of this step is to ensure that the transmission output torque fluctuation is reduced when the motor gradually is reloaded from 0 to the target torque value calculated in the HEV control strategy. Meanwhile the engine output power is gradually reduced to the target power value calculated in the strategy.

Step 7 (Lift the engine speed limit): In this step, the engine speed is released and the engine speed gradually returns to the speed value before the shifting.

4. A Shifting Process Coordination Control Strategy

4.1. Determination and Adjustment of Engine Operating Point during Shifting

When the output torque of the motor drops to 0 and the synchronizer is released, the engine will drive the vehicle alone. According to Equations (4) and (5), the relationship between the target torque and the driving demand torque during the shifting process can be solved as follows:

$$T_{ES} = T_{req} \frac{k_1}{1 + k_1} \quad (20)$$

In order to ensure that the engine can produce enough torque during the shifting process to drive the vehicle alone, the maximum output torque of the engine at the target engine speed $\dot{\theta}_{ES}$ during the shifting process needs to be greater than or equal to the T_{ES} to meet the drive demand torque.

In addition, when the engine is driven alone, the generator needs to run in generation mode to control the engine operating point. And in the shifting process, the motor needs a torque opposite to its own rotation direction for deceleration. It means that the output power is negative, and the generator works in the state of generation. Therefore, the power battery will work in a charging state and the charging power will increase sharply in a short time. To prevent the battery from being damaged and life reduction due to excessive large charging current, the target engine speed during the shifting process should be limited according to the maximum charging power of the power battery and the required torque of the transmission.

When the motor does not start active speed regulation, the output torque and output power are 0 and the generator power is the power battery power. Due to the short shifting process time, it can be considered that the drive demand torque T_{req} and the output shaft speed n_O remain constant. According to Equations (5) and (8), the relationship between the maximum engine speed limit $\dot{\theta}_{ESmax}$ and the maximum battery charging power P_{bcm} during the shifting process can be obtained:

$$\dot{\theta}_{ESmax} = -\frac{KP_{bcm}}{T_{ES}} + \frac{k_1 v_{veh} i_0}{(1 + k_1)r} \quad (21)$$

Considering that the motor needs active speed regulation during the shifting process, a reserved power coefficient K is added to reserve part of the charging power for the active speed regulation stage, and $K = 0.8$ is taken.

Based on the above analysis, the method for determining the target engine speed $\dot{\theta}_{ES}$ is proposed in this paper. $\dot{\theta}_{ES}$, which is shown in Figure 4.

As shown in Figure 4, the strategy for determining the target engine speed can be divided into the following three situations:

If the engine's speed $\dot{\theta}_E < \dot{\theta}_{ESmax}$ before the upshift and the engine's maximum output torque $T_{Emax} \geq T_{ES}$ at the speed $\dot{\theta}_E$, we set $\dot{\theta}_{ES} = \dot{\theta}_E$. In this condition, the engine can drive the vehicle.

If the engine speed $\dot{\theta}_E < \dot{\theta}_{ESmax}$ before the upshift and the engine maximum output torque $T_{Emax} < T_{ES}$ at the speed $\dot{\theta}_E$, the engine torque is not enough to drive the vehicle alone. From the external characteristic curve of the engine shown in Figure 5, the engine can output the maximum torque of 800 Nm at 1200 r/min, and it can be seen from Equation (21) that the smaller the engine speed means the greater the battery charging reserve power. So we set $\dot{\theta}_{ES} = \min(1200, \dot{\theta}_{ESmax})$.

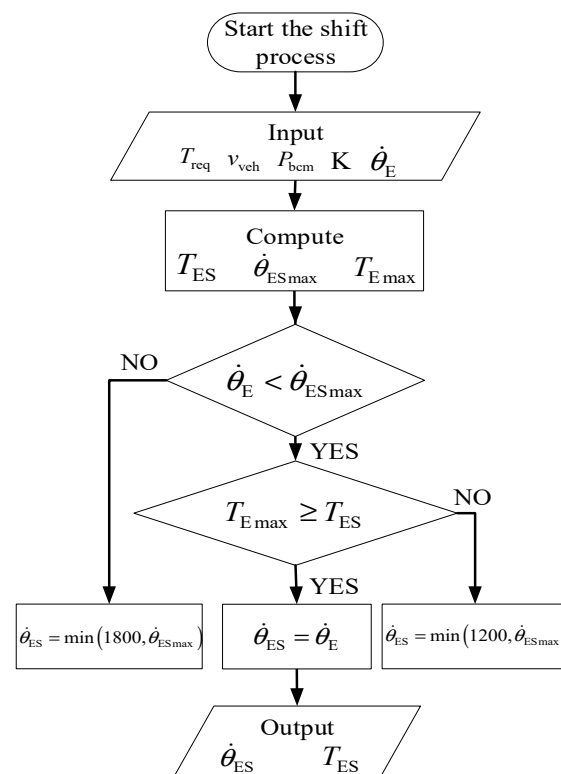


Figure 4. Calculation method of engine target speed during shifting.

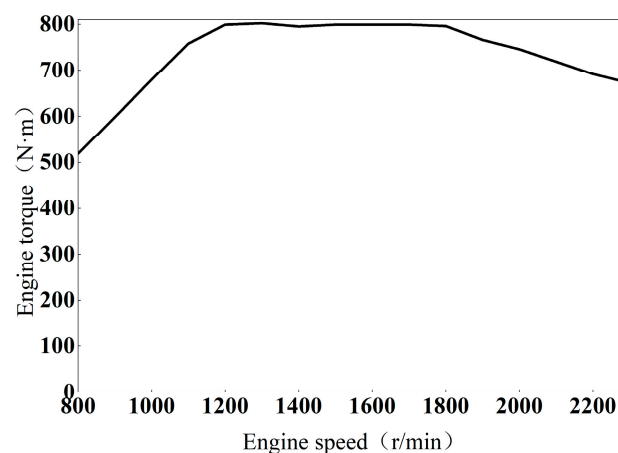


Figure 5. External characteristic of engine.

If the engine speed $\dot{\theta}_E > \dot{\theta}_{ESmax}$ before the upshift, it can be seen from Figure 5 that when the engine speed is greater than 1800 r/min, the maximum output torque gradually decreases. That is, when the speed is greater than 1800 r/min, the motor gradually weakens. So we set $\dot{\theta}_{ES} = \min(1800, \dot{\theta}_{ESmax})$. The flow chart for determining target speed during engine shift is shown in Figure 4.

After entering the first step of the shifting process, the engine target power value is still given by the HEV control strategy, but the engine target operating point is not determined by the economic curve. The target engine speed changes from $\dot{\theta}_E$ to $\dot{\theta}_{ES}$, and the ECU will adjust the output torque of the engine at the same time to control the speed. At this time, since the target power remains unchanged, the target torque also needs to change with the target speed, and the target torque value will be sent to the generator controller unit (GCU) to adjust the engine load.

4.2. A Dynamic Coordinated Control Process Control Strategy

According to the shifting process described in Sections 2 and 3, coordinated torque control of the engine and motor is required in steps 2 and 6. According to Equations (18) and (19), the control of vehicle impact requires the control of the change rate of the output torque of the engine and the motor, so that the ratio of the two torque is kept within a certain range.

In practice, the engine uses speed control. When the target speed of the engine is given, the ECU can use PID control to send a suitable fuel injection signal through the difference between the current speed and the target speed, resulting in a long response time of the engine usually above 500 ms. The response time of the motor to the torque signal is much less than the time of the engine, which is mostly less than 50 ms. Therefore, in the process of torque coordination, the target speed of the engine shifting process should be given first. When the engine output torque responds, the motor compensates the torque fluctuation using its rapid responding characteristics. During the adjustment of the engine operating point, the target value of the torque change rate of the motor is calculated by Equations (18) and (19), and then the target value is limited to achieve the requirement of eliminating impact in the torque coordinated control. In this paper, the following dynamic coordination control strategy is developed:

In the second stage, the engine target speed given by TCU is determined by the strategy proposed in Section 3.1, and the engine target torque signal is calculated by Equation (21). The generator is slowly loaded according to the calculated target torque signal through Equation (15). As the output torque of the generator increases, the actual engine speed will first decrease. After detecting the decrease, ECU will increase the engine fuel injection and increase the torque output to control the engine speed close to the target speed. At the same time, the change rate of the engine is calculated according to the current output torque signal fed back from the ECU, and the target change rate of the motor torque is calculated according to Equation (18), then the output torque of the motor at the next control step is calculated. This signal is sent to the MCU to control the output torque of the motor so that it slowly drops to 0.

The sixth stage is similar to the second stage, the output torque of the generator is reduced by the engine while the target speed is kept unchanged. As the load decreases, the engine speed will increase first. After detecting the increase in the engine speed, the ECU will reduce the engine fuel injection and reduce the torque output to control the engine speed close to the target speed. The current output torque signal change rate of the engine is calculated, and the target torque change rate of the motor is calculated according to Equation (19), and then the output torque of the motor is controlled to slowly rise to the target torque value in HEV mode.

5. Simulation, the Hardware-in-the-Loop (HIL) Test and Result Analysis

5.1. Simulation Model and the HIL Test

Based on MATLAB/Simulink 2020b the simulation model of two-gear power-split hybrid system is established, as shown in Figure 6. The model consists of driver model, controller model, power battery physical model, engine physical model, transmission physical model, motor physical model and vehicle physical model. The vehicle data are shown in Table 2. The simulation is conducted by using fixed-step solver and the simulation step time is 0.001 s.

Based on the simulation model of two-gear power-split hybrid system, a HIL test of the dynamic coordinated control strategy of the system is conducted. A Speedgoat GmbH is adopted to serve as the vehicle and a RapidECU-S2V3 is adopted as the controller in the HIL test. CAN communication is used as a means of communication among the host computer, controller and the Speedgoat. The control step time of the controller is 0.01 s.

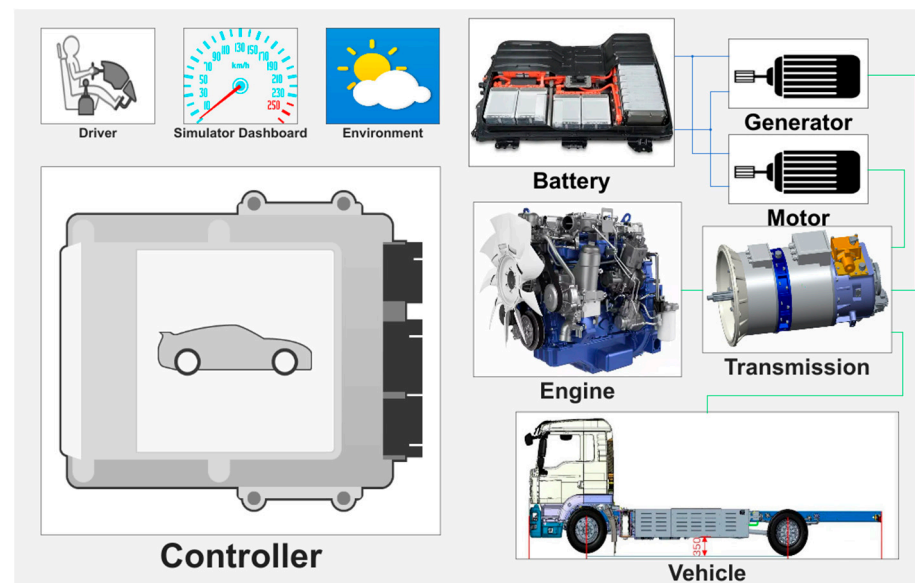


Figure 6. Simulation model of two-gear power-split hybrid system.

Table 2. Parameters of vehicle.

Parameter Name	Numerical Value
Vehicle curb weight m/kg	18,000
Wheel radius r/m	0.51
Rolling resistance coefficient f	0.009
Windward area A/m^2	6.825
Drag coefficient C_d	0.8
Moment of inertia of the engine $J_E/\text{kg}\cdot\text{m}^2$	2.5
Maximum torque of generator (Maximum Power) $N(\text{kW})$	500 (94)
Generator moment of inertia $J_G/\text{kg}\cdot\text{m}^2$	0.1
Maximum torque of motor (Maximum power) $N\cdot\text{m}(\text{kW})$	100 (125)
Moment of inertia of the motor $J_M/\text{kg}\cdot\text{m}^2$	0.1
Characteristic value of coupling mechanism planetary gear k_1	2.16

5.2. Simulation Condition and Result Analysis

A shifting process of slow acceleration with an accelerator pedal value 0.4 is selected for simulation analysis. In the simulation, the shift speed threshold of the motor is set at 3300 r/min. When dynamic coordinated control and engine speed control are not carried out during the shifting process, the engine keeps the working point unchanged during the shifting process, and the output torque change rate of the motor is not limited. The simulation results are as shown in Figures 7 and 8:

When the rule-based control strategy is adopted, the shifting steps and corresponding means are as follows:

1—The torque of the motor decreases rapidly to 0; 2—Synchronizer disconnected. 3—Motor active speed regulation is active. 4—Synchronizer combination is carried.

When there is a dynamic coordination strategy, the shifting steps and corresponding meanings are as follows:

1—Engine speed adjustment. 2—Motor torque reduction process dynamic coordination control. 3—Synchronizer disconnected. 4—Motor active speed regulation. 5—Synchronizer combination. 6—Motor torque recovery process dynamic coordination control.

As shown in Figure 7, the motor reaches the shift speed threshold at 24.57 s and starts to shift. Under the original torque-free control strategy, the transmission completes the shift after 2.36 s and the process ends at 26.93 s. However, after adding the torque control strategy, due to the increase in steps in the shifting process and the excessive consumption

of time in the dynamic coordinated control process of step 2 to ensure the smoothness of the shift, the transmission did not complete the shift until at 32.52 s, which cost 7.95 s.

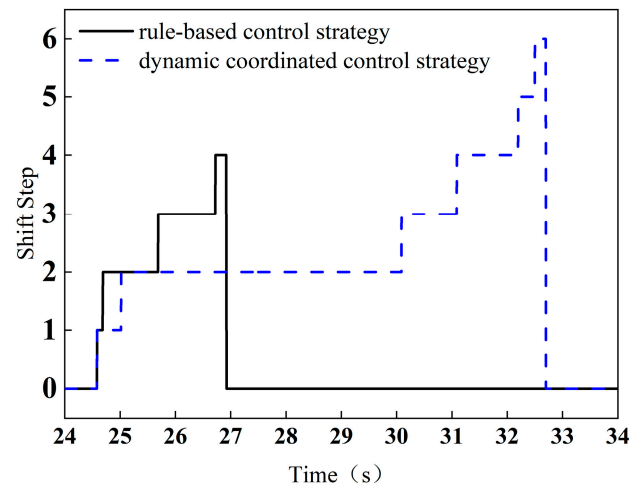


Figure 7. Comparison of shift step.

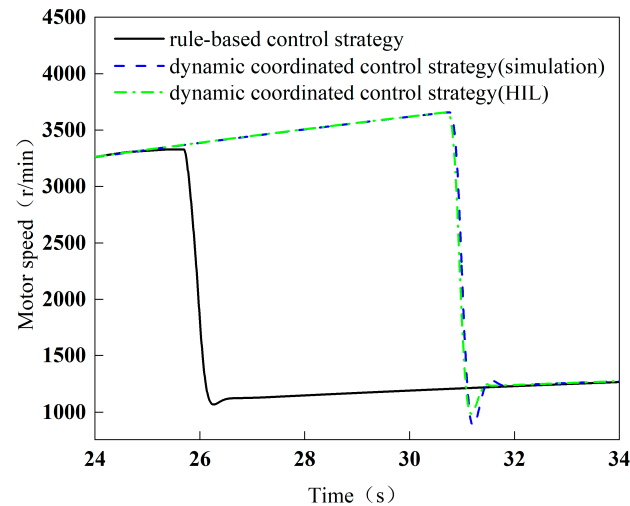


Figure 8. Comparison of motor speed.

The comparison of simulated vehicle speed is shown in Figure 9 and the comparison of simulated vehicle acceleration is shown in Figure 10. Without the dynamic coordinated control strategy, the vehicle acceleration has an obvious decreasing process when the motor is unloaded. After the dynamic coordinated control strategy is added, the acceleration in the whole shifting process slowly decreases with the increase in the speed. However, the acceleration fluctuation range of the whole vehicle is small, which can basically be controlled near the target acceleration. Therefore, the speed hardly fluctuates in the whole process, which improves the dynamic performance during shifting. Due to the different step sizes between simulation and HIL testing, and the limitations of the Simulink model and controller itself, the results of the simulation and the HIL test are different.

According to the comparison of vehicle impact in the simulation as shown in Figure 11, the impact of 1.7450 m/s^3 will be generated in the unloading process of the motor without the dynamic coordinated control strategy. After the dynamic coordinated control strategy is added, the maximum impact of the shifting process is reduced to 0.3433 m/s^3 in the HIL test, and the peak impact is reduced by 80.33%. Therefore, the dynamic coordinated control strategy can significantly reduce the vehicle impact and improve the comfort of shifting.

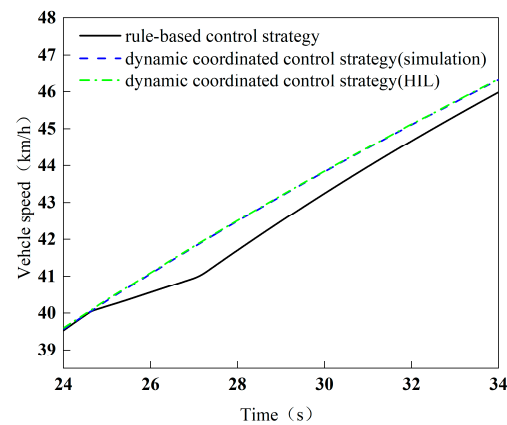


Figure 9. Comparison of vehicle speed.

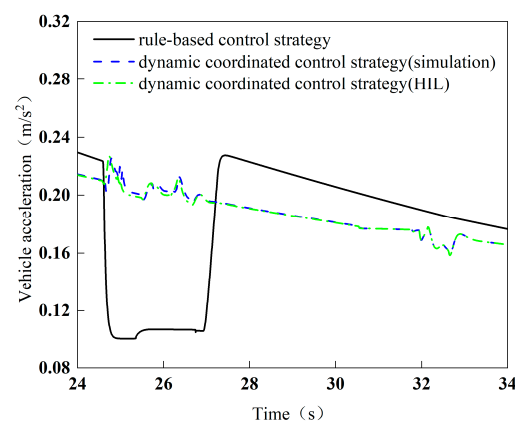


Figure 10. Comparison of vehicle acceleration.

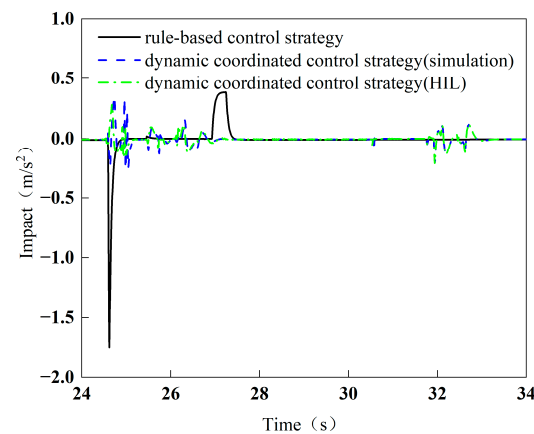


Figure 11. Comparison of vehicle impact.

According to the comparison of engine speed in Figure 12 and engine output torque in Figure 13, TCU will select an appropriate speed in the process of shifting after the dynamic coordinated control strategy is added. The ECU will adjust the engine fuel injection to increase the engine output torque to maintain the engine at the same speed. At the same time, as shown in Figure 14, the torque of the motor will slowly decrease with the increase in the engine torque. However, due to the influence of the speed regulation characteristics of the engine, the output torque will fluctuate during the active speed regulation of the engine in the front and last stages of the gear shifting, and the speed cannot be maintained at a constant as expected during the gear shifting process. These two problems lead to

two impact peaks of approximately 0.4 in Figure 11 and small acceleration fluctuations in Figure 10.

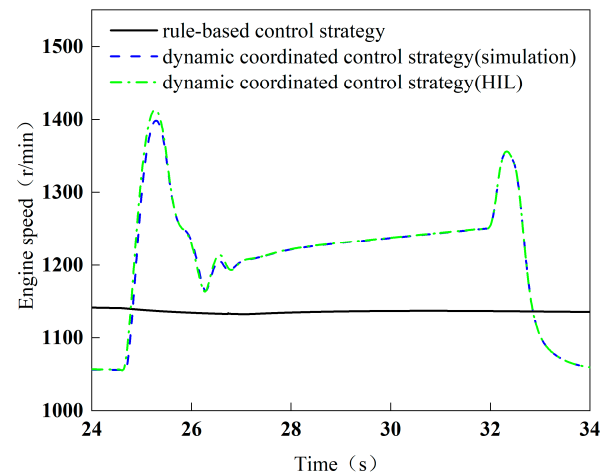


Figure 12. Comparison of engine speed.

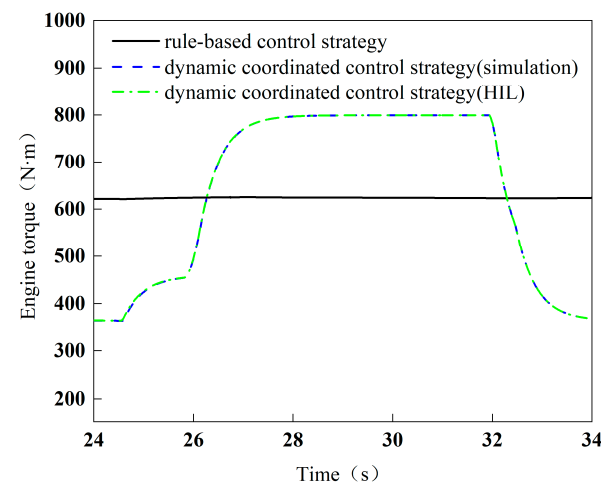


Figure 13. Comparison of engine output torque.

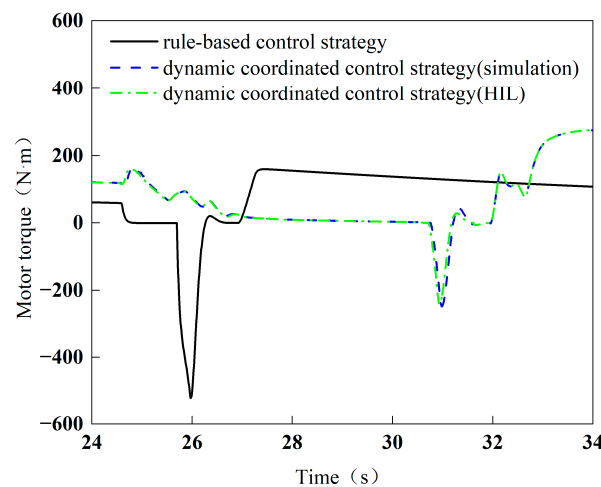


Figure 14. Comparison of motor output torque.

The power of the power battery in the simulation process is shown as Figure 15. It can be seen that during the whole shifting process, the power of the power battery is limited to

the maximum charging and discharging power (-158.4 kW and 217.3 kW). And there is no problem of excessive charging power of the power battery. So the power battery works in safety.

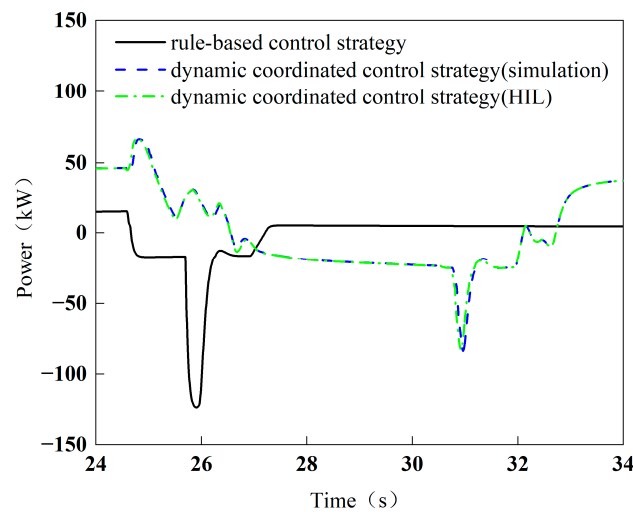


Figure 15. Simulation of power battery power.

Although the shift time increases after the dynamic coordinated control strategy is added, the vehicle acceleration can be kept basically unchanged during the whole shifting process. And the vehicle impact is greatly reduced, ensuring the vehicle power and comfort during the shifting process. Although the coordinated control strategy without a torque coordinate control strategy will significantly reduce the shifting time, the vehicle acceleration will be greatly reduced during the shifting process. And there will be a large peak impact, which cannot guarantee the vehicle dynamics and comfort during the shifting process. In the actual controller of the vehicle, the dynamic coordinated control strategy can be written in the TCU to enable vehicles using two-gear power-split hybrid system to achieve mode switch without power interruption, which can improve the smoothness of driving.

6. Conclusions

In this paper, the gear switching process of a new two-speed power-split hybrid system is studied as follows:

- (1) Based on the dynamic analysis of the two-speed power-split hybrid system, a dynamic model is established. According to the results of dynamic analysis, it is suggested that the engine speed should be controlled at constant in the shifting process to eliminate the influence of engine angular acceleration on vehicle longitudinal acceleration and impact control. And the ratio of the optimal torque change rate between the motor and the engine during the unloading and loading of the motor in the shifting process is proposed.
- (2) The whole shifting process is divided into three stages and seven steps. Considering the limitation of the maximum changing capacity of the power battery and the external characteristics of the engine itself, a method to determine the target engine speed during the shifting process was proposed. According to the difference of response speed between engine and motor, the dynamic coordination control strategy between engine, generator and motor is proposed.
- (3) The simulation results show that the proposed strategy reduces 80.33% of the impact during the mode switch process, the acceleration ability of the vehicle is improved. The ride comfort and power of the vehicle during the mode switch process are guaranteed. At the same time, the engine operating point is adjusted during the single engine driving stage, and the power battery is prevented from high current charging.

- (4) By using the torque compensation strategy, the problem of significant impact on the hybrid system during driving has been improved. The large impact during the mode switch process is decomposed into multiple smaller impacts, which have a certain influence on comfort. However, this impact is so weak that it can be solved by vibration reduction.

Author Contributions: Software and writing—original draft, Q.S.; investigation and writing—review and editing, X.L. (Xueliang Li); validation and visualization, X.L. (Xinlei Liu); conceptualization and methodology, W.W. All authors have read and agreed to the published version of the manuscript.

Funding: This research was funded by the National Natural Science Foundation of China (NSFC), grant number 52102429.

Data Availability Statement: The raw data supporting the conclusions of this article will be made available by the authors on request.

Conflicts of Interest: The authors declare no conflict of interest.

Nomenclature

T_{Mreq}	Drive motor required torque
P_{Ereq}	Engine required power
P_{Breq}	Power battery required power
P_G	Generator power
P_M	Drive motor power
P_{bcm}	Current maximum charging power of the battery
P_{bdcm}	Current maximum discharging power of the battery
v_{veh}	Vehicle speed
F_t	Vehicle driving force
m	Vehicle mass
F_{res}	Vehicle resistance
F_f	Ground rolling resistance
F_w	Wind resistance
F_i	Grade resistance
T_{wheel}	Total torque of driving wheels
T_O	Transmission output torque
i_0	Main reducer transmission ratio
η_0	Main reducer transmission efficiency
r	Tire radius
T_S	Torque of the solar gear
T_C	Torque of the carrier gear
T_R	Torque of the ring gear
T_{OL}	Low-gear output torque
T_{ON}	Neutral gear output torque
T_{OH}	High-gear output torque
T_E	Engine torque
T_G	Generator torque
T_M	Drive motor torque
J_E	Engine moment of inertia
J_G	Generator moment of inertia
J_M	Drive motor moment of inertia
k	Characteristic parameter of the planetary gear

References

1. Su, C.W.; Yuan, X.; Tao, R.; Umar, M. Can new energy vehicles help to achieve carbon neutrality targets. *J. Environ. Manag.* **2021**, *297*, 113348. [\[CrossRef\]](#)
2. Agamloh, E.; von Jouanne, A.; Yokochi, A. An Overview of Electric Machine Trends in Modern Electric Vehicles. *Machines* **2020**, *8*, 20. [\[CrossRef\]](#)
3. De Pinto, S.; Mantriota, G. Power Flows in Compound Transmissions for Hybrid Vehicles. *Machines* **2019**, *7*, 19. [\[CrossRef\]](#)

4. Meisel, J. An Analytic Foundation for the Two-Mode Hybrid-Electric Powertrain with a Comparison to the Single-Mode Toyota Prius THS-II Powertrain. In Proceedings of the SAE World Congress & Exhibition, Detroit, MI, USA, 20–23 April 2009.
5. Wang, Y.; Lü, E.; Lu, H.; Zhang, N.; Zhou, X. Comprehensive design and optimization of an electric vehicle powertrain equipped with a two-speed dual-clutch transmission. *Adv. Mech. Eng.* **2017**, *9*, 1687814016683144. [\[CrossRef\]](#)
6. Hu, M.; Jiang, G.; Fu, C.; Qin, D. Torque coordinated control in engine starting process for a single-motor hybrid electric vehicle. *Adv. Mech. Eng.* **2017**, *9*, 1687814017705965. [\[CrossRef\]](#)
7. He, R.; Tian, X.; Ni, Y.; Xu, Y. Mode transition coordination control for parallel hybrid electric vehicle based on switched system. *Adv. Mech. Eng.* **2017**, *9*, 1687814017715564. [\[CrossRef\]](#)
8. Wang, S.; Xia, B.; He, C.; Zhang, S.; Shi, D. Mode transition control for single-shaft parallel hybrid electric vehicle using model predictive control approach. *Adv. Mech. Eng.* **2018**, *10*, 1687814018775883. [\[CrossRef\]](#)
9. Wang, J.; Cai, Y.; Chen, L.; Shi, D.; Wang, R.; Zhu, Z. Review on multi-power sources dynamic coordinated control of hybrid electric vehicle during driving mode transition process. *Int. J. Energy Res.* **2020**, *44*, 6128–6148. [\[CrossRef\]](#)
10. Yi, T.; Jianqiu, L.; Junzhi, Z.; Fuyuan, Y.; Kexun, Z.; Minggao, Y. Coordinating Control Oriented Research on Algorithm of Engine Torque Estimation for Parallel Hybrid Electric Powertrain System. In Proceedings of the SAE 2004 World Congress & Exhibition, Detroit, MI, USA, 8–11 March 2004.
11. Qin, Z.; Zhang, D.; Han, Y.; Luo, Y. Dynamic coordinated control of a downhill safety assistance system for hybrid electric buses. *Proc. Inst. Mech. Eng. Part D J. Automob. Eng.* **2017**, *231*, 1034–1045. [\[CrossRef\]](#)
12. Koprubasi, K.; Westervelt, E.R.; Rizzoni, G. Toward the Systematic Design of Controllers for Smooth Hybrid Electric Vehicle Mode Changes. In Proceedings of the American Control Conference IEEE 2007, New York, NY, USA, 9–13 July 2007.
13. He, H.; Liu, Z.; Zhu, L.; Liu, X. Dynamic Coordinated Shifting Control of Automated Mechanical Transmissions without a Clutch in a Plug-In Hybrid Electric Vehicle. *Energies* **2012**, *5*, 3094–3109. [\[CrossRef\]](#)
14. Moriya, K.; Ito, Y.; Inaguma, Y.; Sato, E. Design of the surge control method for the electric vehicle powertrain. *SAE Tech. Pap.* **2002**. [\[CrossRef\]](#)
15. Du, B.; Yin, X.; Yang, Y. Robust control of mode transition for a single-motor full hybrid electric vehicle. *Adv. Mech. Eng.* **2017**, *9*, 1687814017717428. [\[CrossRef\]](#)
16. Zeng, X.; Cui, H.; Song, D.; Yang, N.; Liu, T.; Chen, H.; Wang, Y.; Lei, Y. Jerk Analysis of a Power-Split Hybrid Electric Vehicle Based on a Data-Driven Vehicle Dynamics Model. *Energies* **2018**, *11*, 1537. [\[CrossRef\]](#)
17. Sun, J.; Xing, G.; Zhang, C. Data-Driven Predictive Dynamic coordinated Control during Mode Transition Process of Hybrid Electric Vehicles. *Energies* **2017**, *10*, 441. [\[CrossRef\]](#)
18. Glielmo, L.; Iannelli, L.; Vacca, V.; Vasca, F. Gearshift control for automated manual transmissions. *IEEE/ASME Trans. Mechatron.* **2006**, *11*, 17–26. [\[CrossRef\]](#)
19. Hailong, W. Application of Model Predictive Control in Complex Industrial Process. Ph.D. Thesis, Lanzhou University, Lanzhou, China, 2013.
20. Taghavipour, A.; Azad, N.L.; McPhee, J. Real-time predictive control strategy for a plug-in hybrid electric powertrain. *Mechatronics* **2015**, *29*, 13–27. [\[CrossRef\]](#)
21. Beck, R.; Richert, F.; Bollig, A.; Abel, D.; Saenger, S.; Neil, K.; Scholt, T.; Noreikat, K.-E. Model Predictive Control of a Parallel Hybrid Vehicle Drivetrain. In Proceedings of the 44th IEEE Conference on Decision Control/European Control Conference (CCD-ECC), Seville, Spain, 12–15 December 2005; Volume 1–8, pp. 2670–2675.
22. Zeng, X.; Yang, N.; Wang, J.; Song, D.; Zhang, N.; Shang, M.; Liu, J. Predictive-model-based dynamic coordination control strategy for power-split hybrid electric bus. *Mech. Syst. Signal Process.* **2015**, *60*, 785–798. [\[CrossRef\]](#)
23. Tomura, S.; Ito, Y.; Kamichi, K.; Yamanaka, A. Development of vibration reduction motor control for series-parallel hybrid system. In Proceedings of the SAE 2006 World Congress & Exhibition, Detroit, MI, USA, 3–6 April 2006.
24. Wang, Y.; Liu, Z.; Xu, J.; Yan, W. Heterogeneous Network Representation Learning Approach for Ethereum Identity Identification. *IEEE Trans. Comput. Soc. Syst.* **2023**, *10*, 890–899. [\[CrossRef\]](#)
25. Zhao, J.; Lv, Y.; Zeng, Q.; Wan, L. Online Policy Learning-Based Output-Feedback Optimal Control of Continuous-Time Systems. *IEEE Trans. Circuits Syst. II-Express Briefs* **2024**, *71*, 652–656. [\[CrossRef\]](#)

Disclaimer/Publisher’s Note: The statements, opinions and data contained in all publications are solely those of the individual author(s) and contributor(s) and not of MDPI and/or the editor(s). MDPI and/or the editor(s) disclaim responsibility for any injury to people or property resulting from any ideas, methods, instructions or products referred to in the content.